





# Effects of stepwise changes in subjective effort on joint kinematics during the table tennis forehand topspin stroke

 **Yuki Sato** . Department of General Education. National Institute of Technology. Oyama College. Oyama, Japan.  
 **Kengo Wakui**. Division of Humanities and Social Sciences. Niigata University. Niigata, Japan.  
 **Koichiro Miyazaki**. Niigata University. Niigata, Japan.  
**Yukihiko Ushiyama**. Division of Humanities and Social Sciences. Niigata University. Niigata, Japan.

## ABSTRACT

In table tennis forehand topspin strokes, players must regulate output according to rally demands; however, how joint kinematics change over time with subjective effort remains unclear. This study examined phase-dependent changes in pelvic, trunk, and upper-limb joint angles and racket orientation when subjective effort was manipulated in a graded manner. Ten skilled male players performed strokes at 60%, 70%, 80%, 90%, and 100% effort, recorded with motion capture. One-way repeated-measures ANOVA tested effects of effort on peak racket-tip speed, inter-event durations, and joint/racket angles at impact; Statistical Parametric Mapping (SPM) evaluated time-series waveforms. Peak racket-tip speed increased stepwise with effort (significant main effect), whereas inter-event durations showed no significant differences. SPM showed frequent effort-dependent differences in shoulder horizontal flexion/extension and pelvic axial rotation, primarily around impact. At impact, significant main effects were observed mainly in the pelvis, trunk, and proximal upper-limb joints, but not in the forearm, wrist, or racket orientation. During follow-through, effort-related differences emerged in thorax lateral flexion, shoulder internal/external rotation, and racket tilt angle. These findings suggest that increased output with higher effort is achieved mainly through proximal kinematic adjustments and late-phase changes while maintaining distal mechanics and racket configuration at impact. **Keywords:** Performance analysis, Motor control, Motion analysis, Output modulation, Time-series analysis, Racket sports.

### Cite this article as:

Sato, Y., Wakui, K., Miyazaki, K., & Ushiyama, Y. (2026). Effects of stepwise changes in subjective effort on joint kinematics during the table tennis forehand topspin stroke. *Scientific Journal of Sport and Performance*, 5(3), 447-460. <https://doi.org/10.55860/YRCM7402>



**Corresponding author.** Department of General Education. National Institute of Technology. Oyama College. Oyama, Japan.

E-mail: [styk7006@gmail.com](mailto:styk7006@gmail.com)

Submitted for publication February 06, 2026.

Accepted for publication March 16, 2026.

Published March 19, 2026.

[Scientific Journal of Sport and Performance](#). ISSN 2794-0586.

©Asociación Española de Análisis del Rendimiento Deportivo. Alicante. Spain.

doi: <https://doi.org/10.55860/YRCM7402>

## INTRODUCTION

Table tennis requires players to execute accurate strokes in rapid succession, with extremely short reaction times. Therefore, severe temporal constraints constitute a fundamental feature of performance. During rallies, limiting an opponent's available reaction time confers a tactical advantage; thus, increasing the ball speed is a fundamental approach (Lees, 2003). However, topspin strokes must also be executed under the spatial constraint of clearing the net, and kinematic analyses have shown that they simultaneously produce a high racket speed and spin rate (Bańkosz and Winiarski, 2017). The forehand topspin stroke is frequently used as a primary offensive technique (Seemiller and Holowchak, 1997) and generates a high mechanical output through coordinated whole-body movement that sequentially links the trunk, upper limb, and racket. Simultaneously, ball outcomes are influenced by the racket-face orientation at impact (Iino and Kojima, 2009). Accordingly, the forehand topspin stroke constitutes a motor task that requires simultaneous power modulation and precision control, making it well suited for investigation from both kinematic and motor-control perspectives.

The kinematic characteristics of the table tennis forehand topspin stroke have been reported, including joint motions and racket movement patterns during the stroke (Iino and Kojima, 2009; Iino and Kojima, 2011; Kidokoro et al., 2019; Bańkosz and Winiarski, 2025). In high-speed actions, such as striking, throwing, and swinging, velocity generation is typically explained by a proximal-to-distal sequence, in which motion is transferred in a linked manner from proximal to distal segments (Putnam, 1993). Similarly, in table tennis, the rotational motion of the lower trunk has been shown to play an important role in racket-speed development during the forehand topspin stroke. Comparisons across skill levels further indicate that more advanced players exhibit a greater contribution of lower trunk rotation and distinct kinematic features during the racket-acceleration phase (Iino and Kojima, 2009). Using inverse-dynamics approaches, previous studies have also identified the contributions of shoulder internal rotation torque and mechanical energy transfer from the trunk to the upper arm to racket-speed generation (Iino and Kojima, 2011). Moreover, investigations of trunk-upper-limb coordination and muscle activity during table tennis strokes suggest that trunk motion contributes to force production across the stroke (Kondrič et al., 2006; Tsai et al., 2010; Le Mansec et al., 2018).

In competitive table tennis, strokes are not always executed with maximal effort. Instead, players regulate ball speed and spin according to the rally context and tactical intent. This context-dependent output regulation directly supports the consistency of performance and tactical versatility. From a motor control perspective, research has suggested that subjective effort (that is, the effort perceived during movement) may contribute to movement generation, along with externally observable kinematic adjustments. Subjective effort is linked to the central motor command and has been shown to change in parallel with variations in force output and regulation of movement intensity (de Morree et al., 2012). In skilled performance, such variations may manifest as shifts in the movement patterns and coordination (Hashimoto et al., 2021). Consistent with these findings, increases in subjective effort in table tennis coincide with increased ball speed and spin (Sato et al., 2025). Taken together, clarifying how stroke movements are adjusted as subjective effort changes can improve the grasp of output regulation in table tennis and inform approaches to skill acquisition and coaching.

Proximal-to-distal sequencing is widely recognized as a fundamental mechanism for generating end-point velocity in striking and throwing movements (Putnam, 1993; Elliott et al., 1995; Hirashima et al., 2002). In table tennis, three-dimensional kinematic and kinetic analyses have shown that trunk rotation and upper limb motions contribute to racket-speed generation (Iino and Kojima, 2008; Iino et al., 2009; Iino and Kojima, 2011). Despite this body of work, most studies have focused on maximal-effort conditions, skill-level differences, or comparisons across stroke conditions, and investigations addressing output regulation in

relation to subjective effort are scarce. Studies focusing on subjective effort in table tennis have reported increases in ball speed and spin as the effort increases (Sato et al., 2025). However, it is unclear how stroke movements are modified by changing subjective effort, particularly which joints and movement phases exhibit effort-dependent differences when joint kinematics and racket angle are examined as time series.

Accordingly, this study aimed to characterize how three-dimensional joint angles of the pelvis, trunk, and upper-limb joints, together with racket orientation, vary across phases of the table tennis forehand topspin stroke when subjective effort is manipulated at graded levels. We further examined how output regulation accompanying changes in subjective effort is achieved during the stroke by identifying the joints and phases that exhibit effort-dependent differences, with particular attention to changes in stroke duration and adjustment in joint motion. By delineating the correspondence between subjective effort and kinematic alterations, this study seeks to advance the understanding of output regulation in table tennis strokes and provide insights relevant to skill acquisition and coaching.

## MATERIAL AND METHODS

### **Participants**

Ten male table tennis players participated in this study. All participants were right-handed. The mean age, height, and body mass of the participants were  $20.6 \pm 1.4$  years,  $168.7 \pm 6.3$  cm, and  $60.7 \pm 6.8$  kg, respectively. This study was approved by the Ethics Committee of Niigata University (approval number: 2023-2036). Prior to participation, all participants were informed of the purpose and procedures of the experiment, and written informed consent was obtained.

### **Experimental task**

After completing a sufficient self-directed warm-up, the participants performed the experimental trials. The task consisted of forehand topspin strokes, during which the participants were instructed to return balls delivered to the forehand side to the cross-court area (diagonally) of the opponent's court. Participants were instructed as follows: "Assuming that a maximal-effort stroke corresponds to 100%, please perform forehand topspin strokes to the cross-court area at X% effort." The subjective effort was set at five levels: 60%, 70%, 80%, 90%, and 100%. The order of the effort conditions was fixed at 80%, 60%, 90%, 70%, and 100%. This order was selected to avoid potential anchoring effects associated with the 100% effort condition and reduce reference bias arising from consecutive trials at adjacent effort levels (Sato et al., 2025). For each effort condition, five trials that participants judged to match the instructed effort level were included in the analysis. Ball delivery was performed by a single experienced table tennis player who held a Japan Table Tennis Association-certified coaching qualification and was left-handed. The participants used their own rackets, which they routinely employed during training and competition. All rackets were offensive-type rackets equipped with high-tension inverted rubber on both sides (sponge thickness: extra thick). The mean racket mass was  $185.7 \pm 4.6$  g.

### **Measurements**

Body and racket motions were recorded using a motion capture system comprising five infrared cameras (ProReflex MCU240, Qualisys, Sweden) operating at a sampling frequency of 240 Hz. The cameras were arranged around the participant to ensure full coverage of the movement while avoiding interference with the swing motion. To record the instant of ball-racket impact, a digital camera (EX-ZR70; CASIO, Japan) was positioned laterally to the participant and operated at 240 frames per second. To capture upper-body and racket kinematics, spherical retroreflective markers (20 mm in diameter; hereafter referred to as markers) were attached to the anatomical landmarks and racket (Figure 1). Markers were placed on the following

anatomical landmarks: right acromion (AC\_R), left acromion (AC\_L), suprasternal notch (SN), xiphoid process (PX), seventh cervical spinous process (C7), eighth thoracic spinous process (T8), midpoint between the left and right posterior superior iliac spines (PSIS\_M), right anterior superior iliac spine (ASIS\_R), left anterior superior iliac spine (ASIS\_L), right lateral epicondyle of the humerus (EL), right medial epicondyle of the humerus (EM), right radial styloid process (RS), right ulnar styloid process (US), and dorsal aspect of the distal end of the right third metacarpal (MC3). Three markers were attached to the racket: tip (RT), upper region (RU), and lower region (RL). Hereafter, anatomical landmarks and racket markers are referred to using the abbreviations defined earlier. Due to experimental constraints, markers were not placed on the participants' lower limbs. Therefore, all analyses in this study were limited to the upper-body and racket kinematics.

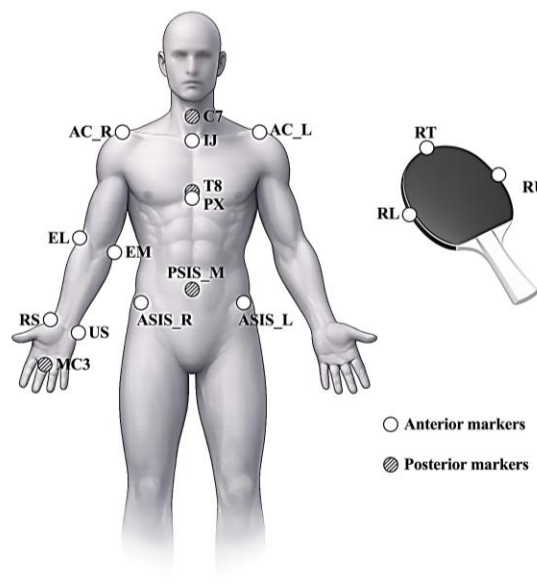


Figure 1. Marker placement on the body and racket.

### Data analysis

A global coordinate system ( $\Sigma_G \equiv O_G - X_G Y_G Z_G$ ) was defined with its origin in the near right corner of the table on the participant's side (from the participant's perspective). The positive  $Z_G$ -axis was defined as the vertical upward direction, the positive  $X_G$ -axis as the ball flight direction (forward from the participant's perspective), and the positive  $Y_G$ -axis as the direction obtained from the cross product of the  $Z_G$ - and  $X_G$ -axes (leftward from the participant's perspective), forming a right-handed coordinate system. The recorded coordinate data were smoothed separately for each axis using a fourth-order, zero-lag (bidirectional) Butterworth low-pass digital filter. The optimal cutoff frequency was determined by residual analysis and ranged from 6–19 Hz. The racket motion during the stroke was calculated from the coordinates of the racket-tip marker, and the stroke interval was defined based on this motion. The instant of ball–racket impact was set to 0 s, and the analysis window was defined from  $-0.6$  to  $+0.3$  s. Within this interval, three key events were identified: T1, defined as the instant when the x-coordinate of the racket tip reached its minimum value (maximum backswing); T2, defined as the instant of ball contact determined using high-speed video footage (impact); and T3, defined as the instant after impact when the racket-tip velocity first reached a local minimum (end of follow-through). The racket-tip velocity was computed as the time derivative of the filtered racket-tip position. To standardize the temporal scale of the stroke, the intervals between T1–T2 and T2–T3 were time-normalized separately for each trial, such that the impact event (T2) was aligned at the same normalized time point across trials.

Time normalization was performed by resampling the data such that T1, T2, and T3 corresponded to 0%, 34%, and 100% of the normalized time scale, respectively. On average, across all trials, T2 occurred at approximately 34% of the stroke cycle. In the present study, continuous motion from T1 to T3 was treated as a single stroke (Figure 2).

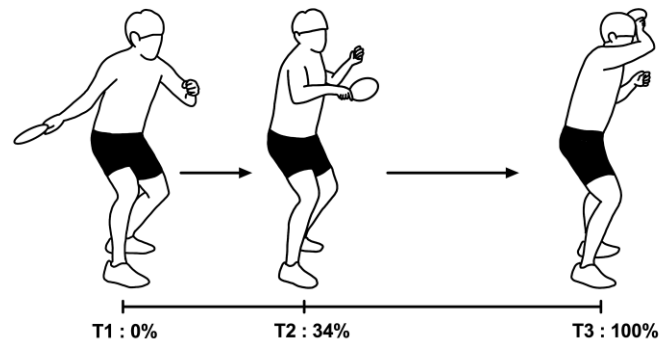


Figure 2. Definition of the stroke interval and key events.

To compute segment kinematics, local coordinate systems for the pelvis, thorax, upper arm, forearm, and hand ( $\Sigma_P$ ,  $\Sigma_T$ ,  $\Sigma_U$ ,  $\Sigma_F$ , and  $\Sigma_H$ ) were defined from the smoothed three-dimensional marker coordinates, with reference to the recommendations of the International Society of Biomechanics (Wu et al., 2002; Wu et al., 2005). The pelvis coordinate system ( $\Sigma_P \equiv O_P - X_P Y_P Z_P$ ) was defined with the origin  $O_P$  as the midpoint of the line segment connecting the midpoint between ASIS\_R and ASIS\_L and PSIS\_M; the  $Z_P$ -axis as the unit vector from ASIS\_L to ASIS\_R (rightward); the  $X_P$ -axis as the unit vector lying in the plane formed by ASIS\_R, ASIS\_L, and PSIS\_M, orthogonal to both the  $Z_P$ -axis and the vector from the ASIS midpoint to PSIS\_M, with the positive direction anterior; and the  $Y_P$ -axis as the cross product of the  $Z_P$ - and  $X_P$ -axes ( $Y_P = Z_P \times X_P$ ), directed superiorly. The thorax coordinate system ( $\Sigma_T \equiv O_T - X_T Y_T Z_T$ ) was defined with the origin  $O_T$  at the SN; the  $Y_T$ -axis as the superiorly directed unit vector from the midpoint between PX and T8 to the midpoint between SN and C7; the  $Z_T$ -axis as the cross product of the  $Y_T$ -axis and the unit vector from SN to C7, directed rightward; and the  $X_T$ -axis as the cross product of the  $Y_T$ - and  $Z_T$ -axes ( $X_T = Y_T \times Z_T$ ), directed anteriorly. The upper arm coordinate system ( $\Sigma_U \equiv O_U - X_U Y_U Z_U$ ) was defined with the origin  $O_U$  at the glenohumeral joint centre (GH), where GH was estimated by translating from AC\_R in a direction perpendicular to the line connecting AC\_R and AC\_L by 1.87% of body height inferiorly and 0.645% of body height anteriorly (Ehara et al., 1998); the  $Y_U$ -axis as the unit vector from the elbow joint centre (EC; midpoint between EM and EL) to GH (proximal direction); the  $X_U$ -axis as the cross product of the  $Y_U$ -axis and the vector from EL to EM, directed anteriorly; and the  $Z_U$ -axis as the cross product of the  $X_U$ - and  $Y_U$ -axes ( $Z_U = X_U \times Y_U$ ), directed laterally for the right upper arm. The forearm coordinate system ( $\Sigma_F \equiv O_F - X_F Y_F Z_F$ ) was defined with the origin  $O_F$  at EC; the  $Y_F$ -axis as the unit vector from the wrist joint centre (WC; midpoint between RS and US) to EC (proximal direction defined as positive); the  $Z_F$ -axis as the cross product of the vector from RS to US and the  $Y_F$ -axis, directed radially; and the  $X_F$ -axis as the cross product of the  $Y_F$ - and  $Z_F$ -axes ( $X_F = Y_F \times Z_F$ ), directed anteriorly (palmar direction). The hand coordinate system ( $\Sigma_H \equiv O_H - X_H Y_H Z_H$ ) was defined with the origin  $O_H$  at WC; the  $Y_H$ -axis as the unit vector from MC3 to WC (proximal direction toward the forearm); the  $Z_H$ -axis as the cross product of the forearm  $Z_F$ -axis and the  $Y_H$ -axis, directed radially (lateral); and the  $X_H$ -axis as the cross product of the  $Y_H$ - and  $Z_H$ -axes ( $X_H = Y_H \times Z_H$ ), directed anteriorly (palmar direction).

Pelvic angles were computed as the relative motion of the pelvis coordinate system ( $\Sigma_P$ ) with respect to the global coordinate system ( $\Sigma_G$ ) using a Z-X'-Y" Cardan rotation sequence. Rotation about the Z-axis

represented pelvic anterior/posterior tilt [extension (+)/flexion (-)], rotation about the X'-axis represented pelvic lateral tilt [left lateral flexion (-)/right lateral flexion (+)], and rotation about the Y"-axis represented pelvic axial rotation [left rotation (+)/right rotation (-)]. Thorax angles were computed as the relative motion of the thorax coordinate system ( $\Sigma_T$ ) with respect to the pelvis coordinate system ( $\Sigma_P$ ) using the same Z-X'-Y" Cardan sequence. Rotation about the Z-axis represented thorax flexion/extension [extension (+)/flexion (-)], rotation about the X'-axis represented thorax lateral flexion [left (-)/right (+)], and rotation about the Y"-axis represented thorax axial rotation [left (+)/right (-)]. Shoulder joint angles were computed as the relative motion of the upper arm coordinate system ( $\Sigma_U$ ) with respect to the thorax coordinate system ( $\Sigma_T$ ) using a Y-X'-Y" Cardan sequence. Rotation about the Y-axis represented shoulder horizontal flexion (+)/horizontal extension (-), rotation about the X'-axis represented shoulder adduction (+)/abduction (-), and rotation about the Y"-axis represented shoulder internal rotation (+)/external rotation (-). The elbow joint angles were computed as the relative motion of the forearm coordinate system ( $\Sigma_F$ ) with respect to the upper arm coordinate system ( $\Sigma_U$ ) using a Z-X'-Y" Cardan sequence. Rotation about the Z-axis represented elbow flexion (+)/extension (-). Rotation about the X'-axis represented the carrying angle (valgus/varus) and was not analysed in this study. Rotation about the Y"-axis represented forearm pronation (+)/supination (-). Wrist joint angles were computed as the relative motion of the hand coordinate system ( $\Sigma_H$ ) with respect to the forearm coordinate system ( $\Sigma_F$ ) using a Z-X'-Y" Cardan sequence. Rotation about the Z-axis represented wrist palmar flexion (+)/dorsiflexion (-), and rotation about the X'-axis represented wrist radial deviation (-)/ulnar deviation (+). Rotation about the Y"-axis was always zero due to constraints of the analysis model and was therefore not analysed. Racket orientation was computed by defining the racket plane using the three racket markers (RT, RU, and RL) and evaluating the direction of the plane normal vector with respect to the global coordinate system. The racket centre was defined as the midpoint between RU and RL. The normal vector was obtained as the cross product of the vector from RU to RL and the vector from the racket centre to RT. Racket orientation was expressed using two components: the horizontal and tilt angles. The horizontal angle was defined as the angle between the projection of the normal vector onto the horizontal plane and the forward axis ( $X_G$ ), which represents the left-right orientation of the racket face. The tilt angle was defined as the elevation angle of the normal vector relative to the horizontal plane, representing the upward-downward inclination of the racket face. Racket-tip speed was computed by time-differentiating the three-dimensional coordinates of the racket-tip marker (RT).

### **Statistical analysis**

For the statistical analyses, mean values were calculated for each participant and each effort condition by averaging the analysed trials (five trials per condition). All tests were two-tailed, and the significance level was set at  $\alpha = .05$ . To examine the effects of effort condition on the peak racket-tip speed, the durations between events (T1-T2, T2-T3, and T1-T3), and the joint angles and racket orientation at impact, a one-way repeated-measures analysis of variance (RM-ANOVA) was performed with effort (five levels) as a within-subject factor. When the assumption of sphericity was violated, the Geisser-Greenhouse correction was applied. When a significant main effect was detected, post hoc pairwise comparisons were conducted using Holm's adjustment for multiple comparisons. To identify the time intervals during which the time-series profiles of joint angles and racket orientation differed across effort conditions, Statistical Parametric Mapping (SPM) was applied using a one-way repeated-measures SPM ANOVA (SPM{F}). For the SPM analyses, each participant's waveform for each effort condition was obtained by averaging the five trials for that condition. Critical thresholds were computed based on random field theory (RFT) to account for the smoothness of the time-series data ( $\alpha = .05$ ), and contiguous supra-threshold regions of the SPM{F} trajectory were extracted as significant intervals. For kinematic variables showing a significant main effect in the one-way repeated-measures SPM ANOVA, post hoc comparisons were performed for all pairwise combinations between conditions (10 pairs) using paired SPM t-tests, with Holm's procedure applied to

control for multiple comparisons. All statistical analyses were performed using GraphPad Prism 10, and SPM analyses were conducted in Python using the spm1d library.

## RESULTS

Peak racket-tip speed increased stepwise with increasing subjective effort conditions (Table 1). The main effect of effort was significant, and post hoc comparisons revealed significant differences between all pairs of effort conditions ( $p < .001$ ). In contrast, no main effect of effort was observed for the inter-event durations (T1–T2, T2–T3, and T1–T3) (T1–T2:  $p = .059$ ; T2–T3:  $p = .149$ ; T1–T3:  $p = .060$ ).

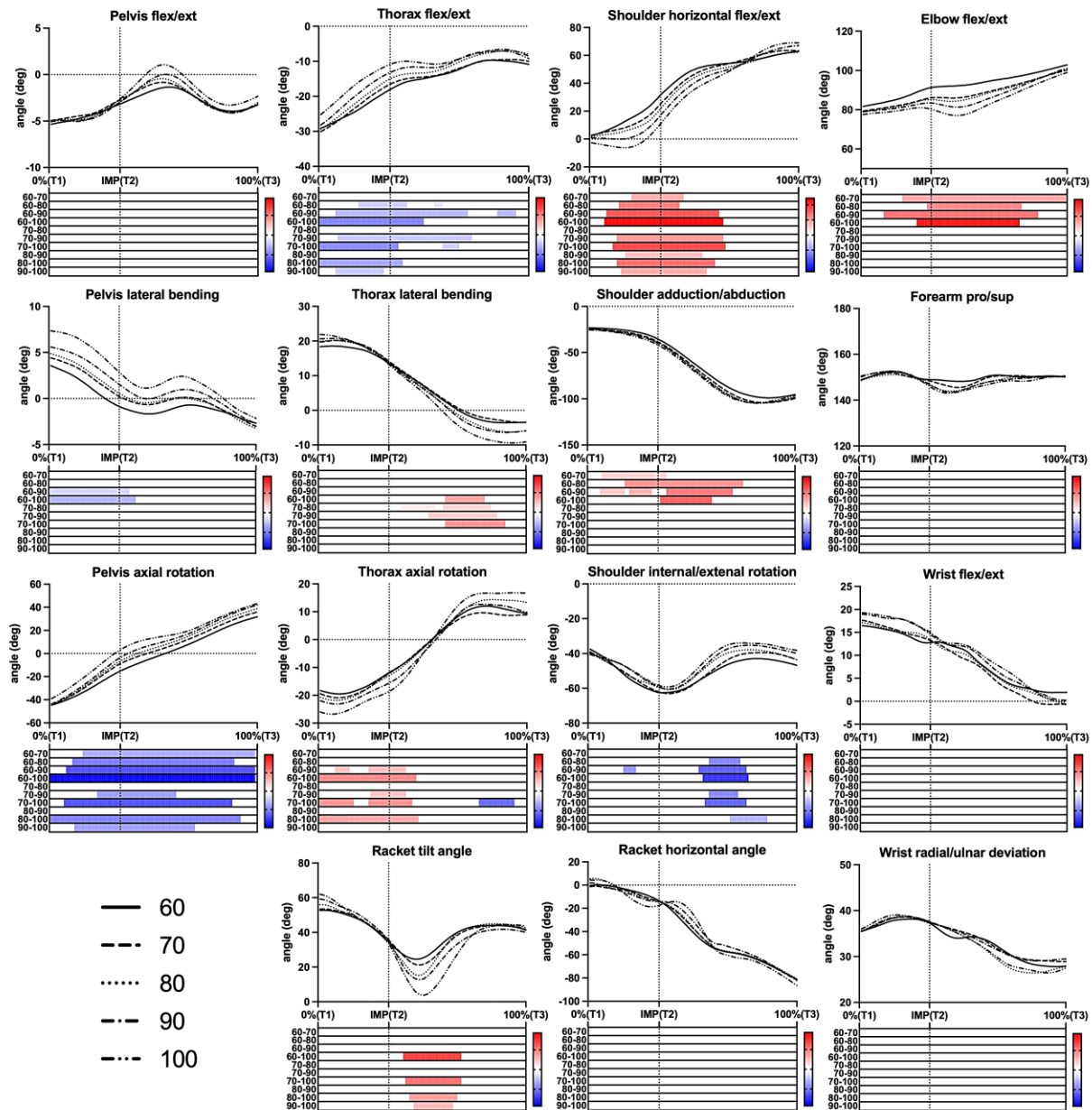


Figure 3. Mean joint-angle waveforms across subjective effort conditions (time-normalized with T1 = 0%, T2 = 34%, and T3 = 100%) and heatmaps indicating significant post hoc SPM results.

Table 1. Peak racket-tip speed and inter-event durations.

	60%	70%	80%	90%	100%	Top: 1 – way repeated-measures ANOVA
	Mean ± SD					Bottom: Compact letter display
Peak racket-tip speed [m/s]	12.72 ± 0.90	13.69 ± 0.78	14.30 ± 0.84	14.83 ± 0.69	15.75 ± 0.69	$p < .001$ , $F(1.97, 17.72) = 114.3$ , $\eta^2 = 0.927$ 60:A, 70:B, 80:C, 90:D, 100:E
T1–T2 [s]	-0.11 ± 0.02	-0.11 ± 0.02	-0.11 ± 0.02	-0.11 ± 0.02	-0.10 ± 0.02	$p = .059$ , $F(2.59, 23.32) = 2.98$ , $\eta^2 = 0.249$ 60:A, 70:A, 80:A, 90:A, 100:A
T2–T3 [s]	0.21 ± 0.02	0.21 ± 0.02	0.20 ± 0.03	0.20 ± 0.03	0.19 ± 0.04	$p = .149$ , $F(1.57, 14.16) = 2.25$ , $\eta^2 = 0.200$ 60:A, 70:A, 80:A, 90:A, 100:A
T1–T3 [s]	0.32 ± 0.03	0.32 ± 0.03	0.31 ± 0.03	0.31 ± 0.03	0.30 ± 0.03	$p = .060$ , $F(1.66, 14.92) = 3.61$ , $\eta^2 = 0.286$ 60:A, 70:A, 80:A, 90:A, 100:A

Table 2. Joint angles at impact.

	Joint angle [°]	60%	70%	80%	90%	100%	Top: 1 - way repeated-measures ANOVA	
		Mean ± SD					Bottom: Compact letter display	
Pelvis	Extension (+)	-3,2 ± 5.7	-2,7 ± 6.2	-2,9 ± 6.6	-3,0 ± 6.3	-2,6 ± 7.0	$p = .818$ , $F(1.54, 13.85) = 0.14$ , $\eta^2 = 0.015$ 60:A, 70:A, 80:A, 90:A, 100:A	
	Flexion (-)							
	Left lateral bending (-)	-0,9 ± 2.6	0,2 ± 3.2	0,5 ± 3.0	1,5 ± 3.0	2,9 ± 2.8	$p = .002$ , $F(1.96, 17.67) = 9.35$ , $\eta^2 = 0.510$ 60:A, 70:AB, 80:AB, 90:B, 100:B	
	Right lateral bending (+)							
	Left rotation (+)	-15,2 ± 10.9	-8,8 ± 7.8	-6,5 ± 11.4	-3,6 ± 10.1	3,1 ± 9.2	$p < .001$ , $F(2.99, 26.96) = 46.51$ , $\eta^2 = 0.838$ 60:A, 70:B, 80:BC, 90:C, 100:D	
Thorax	Right rotation (-)							
	Extension (+)	-18,1 ± 12.7	-16,5 ± 12.8	-15,0 ± 13.7	-13,2 ± 12.7	-10,9 ± 12.7	$p < .001$ , $F(1.71, 15.42) = 19.46$ , $\eta^2 = 0.684$ 60:A, 70:AB, 80:BC, 90:CD, 100:D	
	Flexion (-)							
	Left lateral bending (-)	13,6 ± 3.0	14,1 ± 3.2	13,3 ± 2.8	13,7 ± 3.5	13,3 ± 4.3	$p = .522$ , $F(2.33, 20.99) = 0.71$ , $\eta^2 = 0.073$ 60:A, 70:A, 80:A, 90:A, 100:A	
	Right lateral bending (+)							
Shoulder	Left rotation (+)	-11,8 ± 4.4	-12,1 ± 5.2	-12,9 ± 4.2	-15,5 ± 4.4	-18,6 ± 4.5	$p < .001$ , $F(2.50, 22.51) = 24.92$ , $\eta^2 = 0.735$ 60:A, 70:A, 80:AB, 90:BC, 100:C	
	Right rotation (-)							
	Horizontal flexion (+)	31,7 ± 12.2	25,4 ± 10.6	21,9 ± 14.8	17,2 ± 14.8	11,1 ± 15.9	$p < .001$ , $F(2.44, 22.00) = 43.99$ , $\eta^2 = 0.830$ 60:A, 70:B, 80:B, 90:C, 100:D	
	Horizontal extension (-)							
	Adduction (+)	-35,4 ± 10.4	-38,5 ± 10.3	-39,7 ± 12.5	-39,9 ± 9.0	-41,9 ± 10.3	$p = .021$ , $F(2.00, 18.01) = 4.79$ , $\eta^2 = 0.347$ 60:A, 70:B, 80:B, 90:AB, 100:AB	
Elbow	Abduction (-)							
	Internal rotation (+)	-62,5 ± 14.5	-62,2 ± 14.5	-59,6 ± 15.0	-59,3 ± 16.0	-58,4 ± 16.7	$p = .017$ , $F(2.46, 22.10) = 4.53$ , $\eta^2 = 0.335$ 60:A, 70:A, 80:A, 90:A, 100:A	
	External rotation (-)							
	Flexion (+)	91,3 ± 10.7	86,1 ± 9.4	85,2 ± 10.8	83,5 ± 10.6	80,3 ± 9.0	$p = .001$ , $F(1.92, 17.30) = 10.63$ , $\eta^2 = 0.541$ 60:A, 70:B, 80:B, 90:B, 100:B	
	Extension (-)							
Forearm	Pronation (+)	149,0 ± 12.5	148,5 ± 12.6	146,7 ± 12.7	147,1 ± 13.5	146,2 ± 13.2	$p = .218$ , $F(1.82, 16.40) = 1.68$ , $\eta^2 = 0.157$ 60:A, 70:A, 80:A, 90:A, 100:A	
	Supination (-)							
Wrist	Palmar flexion (+)	12,7 ± 11.6	13,2 ± 11.2	13,3 ± 9.9	15,0 ± 10.9	14,6 ± 9.8	$p = .406$ , $F(1.61, 14.47) = 0.90$ , $\eta^2 = 0.091$ 60:A, 70:A, 80:A, 90:A, 100:A	
	Dorsiflexion (-)							
	Radial deviation (-)	37,3 ± 6.1	37,6 ± 5.8	37,3 ± 5.8	37,5 ± 6.1	37,5 ± 5.8	$p = .747$ , $F(2.43, 21.90) = 0.35$ , $\eta^2 = 0.038$ 60:A, 70:A, 80:A, 90:A, 100:A	
	Ulnar deviation (+)							
Racket	Horizontal	Leftward rotation (+)	-14,1 ± 6.8	-16,4 ± 10.9	-17,0 ± 13.9	-15,3 ± 12.2	-11,0 ± 18.5	$p = .549$ , $F(1.41, 12.71) = 0.51$ , $\eta^2 = 0.054$ 60:A, 70:A, 80:A, 90:A, 100:A
		Rightward rotation (-)						
	Tilt	Upward (+)	34,6 ± 3.2	35,2 ± 4.9	33,5 ± 1.8	36,0 ± 4.6	34,6 ± 2.0	$p = .280$ , $F(1.49, 13.36) = 1.37$ , $\eta^2 = 0.132$ 60:A, 70:A, 80:A, 90:A, 100:A
		Downward (-)						

Figure 3 shows the mean time-normalized waveforms of the joint angles for each subjective effort condition (T1 = 0%, T2 = 34%, T3 = 100%), together with a heatmap summarizing the condition pairs and time intervals that exhibited significant differences in the post hoc analyses ( $p < .05$ ). In the heatmap, the colour indicates the mean difference within significant intervals (A – B), with red denoting  $A > B$  and blue denoting  $A < B$ ; darker colours indicate larger differences within the corresponding intervals. Post hoc comparisons revealed that the largest number of significant condition pairs occurred for shoulder horizontal flexion/extension and pelvic axial rotation. For shoulder horizontal flexion/extension, significant differences were observed for nine pairs, excluding the comparison between 70% and 80%, and these differences were primarily distributed around the impact phase. For pelvic axial rotation, significant differences were observed in eight pairs, with differences broadly distributed from pre-impact to T3. Multiple significant condition pairs were also observed for thorax flexion/extension and shoulder internal/external rotation; differences in thorax flexion/extension were concentrated around the impact, whereas differences in shoulder internal/external rotation were mainly observed after impact. In contrast, several variables showed significant differences for only a limited number of pairs. Pelvic lateral flexion differed significantly between 60% and 90–100% efforts. For elbow flexion/extension, significant differences were observed between 60% and the other conditions (70–100%). Thorax lateral flexion showed differences after impact, whereas thorax axial rotation differed primarily from pre-impact to around the time of impact. For the racket tilt angle, significant differences were observed after impact between 100% and the other conditions (60–90%).

At impact, significant main effects of subjective effort were observed for pelvic lateral flexion and axial rotation, thorax flexion/extension and axial rotation, shoulder horizontal flexion/extension and abduction/adduction, and elbow flexion/extension (Table 2). Post hoc comparisons showed that pelvic lateral flexion increased toward right lateral flexion with increasing effort; the 60% condition was smaller than the high-effort conditions (90–100%) ( $p = .002$ ). Pelvic axial rotation increased toward left rotation with increasing effort; the 60% condition was smaller than the other conditions (70–100%) (all  $p < .001$ ). Thorax flexion/extension shifted toward a less flexed posture with increasing effort; the 60% condition was smaller than the moderate-to-high effort conditions (80–100%) (all  $p < .001$ ). Thorax axial rotation shifted toward right rotation with increasing effort; the low-to-moderate effort conditions (60–70%) were greater than the high-effort conditions (90–100%) (all  $p < .001$ ). Both shoulder horizontal flexion/extension and elbow flexion/extension decreased with increasing effort, and the low-effort conditions were greater than the high-effort conditions ( $p < .001$  and  $p = .001$ , respectively). For shoulder abduction/adduction, the 60% condition was greater than the 70–80% conditions ( $p = .021$ ). Although a significant main effect of effort was observed for shoulder internal/external rotation, no significant between-condition differences were detected in post hoc comparisons at impact. No significant effects of effort were found for the remaining angles (pelvic flexion/extension, thorax lateral flexion, forearm pronation/supination, wrist angles, or racket orientation).

## DISCUSSION

This study aimed to determine how the three-dimensional joint angles of the pelvis, trunk, and upper limb joints, as well as racket orientation, change when subjective effort is manipulated at graded levels during the table tennis forehand topspin stroke. The peak racket-tip speed increased stepwise as the subjective effort increased. The inter-event timing within the stroke did not vary with effort. Time-series analyses showed that the effort-related differences were not uniform across the upper body. These differences were most pronounced in pelvic axial rotation and shoulder horizontal flexion/extension. At impact, effort-dependent differences were evident mainly in the pelvis, trunk, and proximal upper limb joints. No significant differences were observed in the forearm, wrist, or racket orientation. Together, these results indicate that a higher racket

speed with increasing effort is achieved without changes in stroke timing. This increase was primarily expressed through kinematic adjustments in the thorax and proximal upper limb.

The racket-tip speed increased across the effort conditions in this study. The inter-event timing during the stroke remained unchanged. Subjective effort indexes the perceived level of effort required during movement. Subjective effort has been linked to the central motor command (de Morree et al., 2012). Thus, the effort-related increase in output may have been achieved by increasing the kinematic magnitudes within the same temporal window. Proximal segment motion is known to influence distal end-point velocity generation (Putnam, 1993). Effort-dependent differences were most pronounced in pelvic axial rotation and shoulder horizontal flexion/extension. This pattern suggests that effort regulation was implemented without altering the temporal structure of the movement. This also suggests the modulation of the proximal segment motion magnitude while preserving the overall movement pattern. In the forehand topspin, higher-level players showed greater contributions of lower trunk rotation and distinct racket acceleration properties. These findings indicate that trunk motion contributes to racket speed generation (Iino and Kojima, 2009). The present results are consistent with this view. Speed regulation has been observed to cause changes in proximal segment kinematics. Lumbar and pelvic kinematics can change over time across stroke direction conditions (He et al., 2023). This evidence is consistent with pelvic axial rotation serving as an adjustable component in response to situational demands. In contrast, studies focusing on stroke duration differences report that fast and slow strokes differ in the stroke time itself. They also reported concomitant changes in joint kinematics and ball effects (Tian and Xiao, 2024). Here, the racket-tip speed increased stepwise despite no differences in inter-event timing. This finding indicates output regulation without modifying the temporal structure. This also indicates that regulation was expressed mainly as proximal-segment kinematic adjustments. The SPM results further localized effort-dependent differences around the impact. Pelvic axial rotation and shoulder horizontal flexion/extension also changed stepwise with increasing impact effort. This pattern suggests the modulation of proximal motion with effort. This particularly implicates the acceleration phase into the impact.

Time-series analyses also showed that effort-related adjustments were not restricted to the velocity generation phase around the impact. The SPM results in Figure 3 identified significant between-condition differences, mainly after impact (after T2) during follow-through. These effects were observed in thorax lateral flexion, shoulder internal/external rotation, and racket tilt angle. Significant intervals tended to occur in comparisons that included the 100% condition. This post-impact clustering suggests a downstream consequence of greater output with increased effort. The post-impact swing likely increased. Therefore, the follow-through movement pattern may have shifted. Accordingly, the follow-through differences are better attributed to post-contact dynamics than to the kinematics at impact itself. This may reflect greater residual momentum after ball contact. They may also reflect differences in the convergence of movement after impact. Follow-through has been reported to indirectly reflect overall stroke stability. It has also been reported to facilitate a smooth transition to subsequent actions (Lees, 2003; Kondrič et al., 2006). Thus, the effort-dependent differences observed during follow-through can be interpreted as movement elaboration resulting from a greater output under high-effort conditions. These can also be interpreted as differences in the kinematic characteristics during the latter part of the stroke.

Effort-dependent adjustments in the present study emerged mainly in the trunk and proximal upper limbs. They also appeared during the follow-through. In contrast, no significant differences were detected in forearm, wrist, or racket orientation at impact. This pattern may reflect the task constraints specific to table tennis strokes. Large changes in distal joint kinematics or racket orientation at impact are likely to impair the accuracy of the stroke. Thus, even when the effort varies, players may preserve the impact configuration.

Speed regulation can then be implemented through adjustments at other joints. Prior kinematic work on the forehand topspin has shown that the contribution of lower trunk rotation varies across performance levels and stroke conditions. Differences have also been shown in the characteristics of the racket acceleration phase (Iino and Kojima, 2009). In addition, shoulder internal rotation torque and mechanical energy transfer from the trunk to the upper arm contribute to racket-speed generation (Iino and Kojima, 2011). Skilled players in high-speed interceptive tasks can also maintain stable outcomes through the use of online information and compensatory adjustments (Bootsma and van Wieringen, 1990; Bootsma et al., 2010). The present combination of preserved distal/racket configuration at impact and proximal kinematic change is consistent with the control framework. Together, the effort-related modulation of speed generation via proximal segment motion and the follow-through changes in thorax lateral flexion, shoulder internal/external rotation, and racket tilt angle may act in a complementary manner. These effects may reflect a regulation strategy that varies racket speed while maintaining the distal mechanics and racket configuration at impact.

This study had several limitations. We did not directly quantify lower limb motion or muscle activity. Thus, the effort-related increase in output cannot be linked to specific activation patterns or mechanical loads. The order of the effort conditions was fixed. Therefore, the order effects may have contributed to the observed effort effects. Our analyses were limited to upper-body and racket kinematics. Accordingly, we cannot infer the contribution of whole-body kinetic chain mechanisms, including lower limb actions and ground reaction forces. Despite these constraints, the data suggest a characteristic regulation pattern. Distal mechanics and racket orientation at impact showed no significant differences across effort levels. Speed regulation instead appeared to concentrate in proximal-segment motion and the latter phase of the stroke. These findings refine understanding of movement regulation strategies in table tennis strokes. They also carry practical implications for coaching. Proximal-segment motion emerges as a key target when training graded regulation of racket speed. Subjective effort offers a simple way to scale output without specialized equipment. It may support practice tasks that vary speed while preserving impact technique. One example is a drill that increases subjective effort from 60% to 100% while maintaining the same stroke mechanics and target placement. Such a drill could promote speed regulation through trunk rotation and shoulder-related motion. It could also limit excessive changes in distal mechanics and racket orientation.

## CONCLUSIONS

This study quantified time-series changes in pelvis, thorax, and upper-limb joint angles, as well as racket orientation, during the table tennis forehand topspin stroke across graded levels of subjective effort. Peak racket-tip speed increased stepwise with effort. It differed significantly across all effort conditions. In contrast, inter-event durations (T1–T2, T2–T3, and T1–T3) showed no significant differences. Time-series analyses showed that effort-related differences were not uniform across the upper body. They were most pronounced in shoulder horizontal flexion/extension and pelvic axial rotation. These differences clustered mainly around the impact phase. At impact, effort-dependent differences emerged primarily in the pelvis, thorax, and proximal upper-limb joints angles. No significant differences were detected in the forearm, wrist, or racket orientation. During follow-through, effort-related differences appeared in thorax lateral flexion, shoulder internal/external rotation, and racket tilt angle. This pattern suggests distinct movement elaboration under high-effort conditions. Overall, skilled players may increase output with higher effort without altering the temporal structure of the stroke. This may be achieved mainly through kinematic adjustments in the thorax and proximal upper limb. It may also be achieved through changes in movement characteristics during the latter phase of the stroke. Distal mechanics and racket configuration at impact may remain relatively stable.

## AUTHOR CONTRIBUTIONS

YS (Corresponding Author) contributed to Conceptualization, Methodology, Investigation, Formal analysis, and Writing – Original Draft. He also contributed to Writing – Review & Editing and coordinated the overall research process. KW contributed to Investigation, provided Methodology advice, assisted in Validation, and participated in Writing – Review & Editing. KM contributed to Investigation and participated in Writing – Review & Editing. YU contributed to Supervision, Validation, and Writing – Review & Editing. All authors reviewed and approved the final version of the manuscript.

## SUPPORTING AGENCIES

No funding agencies were reported by the authors.

## DISCLOSURE STATEMENT

No potential conflict of interest was reported by the authors.

## ACKNOWLEDGEMENTS

The authors would like to thank all participants for their cooperation throughout the experiment. This study was conducted in accordance with the current laws of Japan.

## REFERENCES

- Bańkosz, Z., & Winiarski, S. (2017). The kinematics of table tennis racquet: differences between topspin strokes. *J. Sports. Med. Phys. Fit.*, 57, 202-213. <https://doi.org/10.23736/S0022-4707.16.06104-1>
- Bańkosz Z, Winiarski S. (2020). Kinematic Parameters of Topspin Forehand in Table Tennis and Their Inter- and Intra-Individual Variability. *J Sports Sci Med.*, 19(1), 138-148. <https://doi.org/10.1155/2020/8413948>
- Bańkosz Z, Winiarski S. (2025). Kinematics of Topspin Stroke Combinations in Table Tennis and its Inter-Individual Variability. *J Sports Sci Med.*, 24(2), 311-325. <https://doi.org/10.52082/jssm.2025.311>
- Bootsma, R. J., & van Wieringen, P. C. W. (1990). Timing an attacking forehand drive in table tennis. *J Exp Psychol Hum Percept Perform.*, 16(1), 21-29. <https://doi.org/10.1037/0096-1523.16.1.21>
- Bootsma, R. J., Fernandez, L., Morice, A. H., & Montagne, G. (2010). Top-level players' visual control of interceptive actions: Bootsma and van Wieringen (1990) 20 years later. *J Exp Psychol Hum Percept Perform.*, 36(4), 1056-1066. <https://doi.org/10.1037/a0019327>
- De Morree, H. M., Klein, C., & Marcora, S. M. (2012). Perception of effort reflects central motor command during movement execution. *Psychophysiology*, 49(9), 1242-1253. <https://doi.org/10.1111/j.1469-8986.2012.01399.x>
- Ehara, Y., Beppu, M., Nomura, S., Kunimi, Y., Kouya, N., Tsutiya, T., Fujinawa, M., & Hoshi, M. (1998). Biomechanical analysis of the force produced in the shoulder during baseball pitching. *Biomechanisms*. 14, 39-48. <https://doi.org/10.3951/biomechanisms.14.39>
- Elliott, B. C., Marshall, R. N., & Noffal, G. J. (1995). Contributions of Upper Limb Segment Rotations during the Power Serve in Tennis. *J Appl Biomech.*, 11(4), 433-442. <https://doi.org/10.1123/jab.11.4.433>
- Hashimoto, T., Takiyama, K., Miki, T., Kobayashi, H., Nasu, D., Ijiri, T., Kuwata, M., Kashino, M., & Nakazawa, K. (2021). Effort-dependent effects on uniform and diverse muscle activity features in skilled pitching. *Sci. Rep.*, 11, 8211. <https://doi.org/10.1038/s41598-021-87614-z>

- Hirashima, M., Kadota, H., Sakurai, S., Kudo, K., & Ohtsuki, T. (2002). Sequential muscle activity and its functional role in fast movement. *J Sports Sci.*, 20(4), 301-310. <https://doi.org/10.1080/026404102753576071>
- He, Y., Liang, M., Fang, Y., Fekete, G., Baker, J. S., & Gu, Y. (2023). Lumbar and pelvis movement comparison between cross-court and long-line topspin forehand in table tennis: Based on musculoskeletal model. *Frontiers in Bioengineering and Biotechnology*, 11, 1185177. <https://doi.org/10.3389/fbioe.2023.1185177>
- Le Mansec, Y., Dorel, S., Hug, F., & Jubeau, M. (2018). Lower limb muscle activity during table tennis strokes. *Sports Biomech.*, 17(4), 442-452. <https://doi.org/10.1080/14763141.2017.1354064>
- Lino, Y., Mori, T., & Kojima, T. (2008). Contributions of upper limb rotations to racket velocity in table tennis backhands against topspin and backspin. *J Sports Sci.*, 26(3), 287-293. <https://doi.org/10.1080/02640410701501705>
- Lino, Y., & Kojima, T. (2009). Kinematics of table tennis topspin forehands: effects of performance level and ball spin. *J Sports Sci.*, 27(12), 1311-1322. <https://doi.org/10.1080/02640410903264458>
- Lino, Y., & Kojima, T. (2011). Kinetics of the upper limb during table tennis topspin forehands in advanced and intermediate players. *Sports Biomech.*, 10(4), 361-377. <https://doi.org/10.1080/14763141.2011.629304>
- Kidokoro, S., Inaba Y., Yoshida K., Yamada K., & Ozaki H. (2018). Characteristics of three different topspin forehands in Japanese elite table tennis players: Impact for generating the batted ball with high initial velocity. *Jpn J Biomech Sports Exerc.*, 22(4), 152-166. [https://doi.org/10.32226/jjbse.22\\_2018\\_003](https://doi.org/10.32226/jjbse.22_2018_003)
- Kidokoro, S., Inaba Y., Yoshida K., Yamada K., & Ozaki H. (2019). The influence of shoulder and torso joint mobility on three different topspin forehands in a situation accompanied by body movement in Japanese elite table tennis players. *Jpn J Phys Educ Hlth Sport Sci.*, 64(1), 169-185. <https://doi.org/10.5432/ijpehss.18029>
- Kondrič, M., Furjan-Mandić, G., & Medved, V. (2006). Myoelectric comparison of table tennis forehand stroke using different ball sizes. *Acta Univ. Palacki. Olomuc., Gymn.*, 36(4), 25-28.
- Lees, A. (2003). Science and the major racket sports: A review. *J. Sports Sci.*, 21(9), 707-732. <https://doi.org/10.1080/0264041031000140275>
- Putnam, C. A. (1993). Sequential motions of body segments in striking and throwing skills: Descriptions and explanations. *J Biomech.*, 26(1), 125-135. [https://doi.org/10.1016/0021-9290\(93\)90084-R](https://doi.org/10.1016/0021-9290(93)90084-R)
- Sato, Y., Wakui, K., Miyazaki, K., & Ushiyama, Y. (2025). Effects of subjective effort on ball speed and spin in table tennis forehand topspin strokes. *International Journal of Sports Science & Coaching*, 1-11. <https://doi.org/10.1177/17479541251380169>
- Seemiller, D., & Holowchak, M. A. (1997). *Winning table tennis*. Human Kinetics.
- Tian, J., & Xiao, Y. (2024). Research on the difference of stroke characteristics and stroke effect between different stroke duration of table tennis players. *Scientific Reports*, 14, 25405. <https://doi.org/10.1038/s41598-024-76802-2>
- Tsai, C.-L., Pan, K.-M., Huang, K.-S., Chang, T.-J., Hsueh, Y.-C., Wang, L.-M., & Chang, S.-S. (2010). The surface EMG activity of the upper limb muscles in table tennis forehand drives. *Int. Symp. Biomech. Sports: Conf. Proc. Arch.*, 28, 1-4.
- Wu, G., Siegler, S., Allard, P., Kirtley, C., Leardini, A., Rosenbaum, D., Whittle, M., D'Lima, D. D., Cristofolini, L., Witte, H., Schmid, O., Stokes, I., & Standardization and Terminology Committee of the International Society of Biomechanics (2002). ISB recommendation on definitions of joint coordinate system of various joints for the reporting of human joint motion--part I: ankle, hip, and spine. *International Society of Biomechanics. Journal of biomechanics*, 35(4), 543-548. [https://doi.org/10.1016/S0021-9290\(01\)00222-6](https://doi.org/10.1016/S0021-9290(01)00222-6)

Wu, G., van der Helm, F. C., Veeger, H. E., Makhsous, M., Van Roy, P., Anglin, C., Nagels, J., Karduna, A. R., McQuade, K., Wang, X., Werner, F. W., Buchholz, B., & International Society of Biomechanics (2005). ISB recommendation on definitions of joint coordinate systems of various joints for the reporting of human joint motion--Part II: shoulder, elbow, wrist and hand. *Journal of biomechanics*, 38(5), 981-992. <https://doi.org/10.1016/j.jbiomech.2004.05.042>



This work is licensed under a [Attribution-NonCommercial-ShareAlike 4.0 International](https://creativecommons.org/licenses/by-nc-sa/4.0/) (CC BY-NC-SA 4.0).